# Dynamic Mechanical Properties and Morphology of Polypropylene/Maleated Polypropylene Blends

PENTTI JÄRVELÄ,[1,*] LI SHUCAI,[1,†] and PIRKKO JÄRVELÄ[2]

[1]Tampere University of Technology, Institute of Plastics Technology, P.O. Box 589, 33101 Tampere, and [2]VTT Chemical Technology, Polymer and Fibre Technology, P.O. Box 1402, 33101 Tampere, Finland

SYNOPSIS

The dynamic mechanical properties of both homopolypropylene (PPVC)/Maleated Polypropylene (PP-*g*-MA) and ethylene-propylene block copolymer (PPSC)/Maleated Polypropylene (PP-*g*-MA) blends have been studied by using a dynamic mechanical thermal analyzer (PL-DMTA MKII) over a wide temperature range, covering a frequency zone from 0.3 to 30 Hz. With increasing content of PP-*g*-MA, $\alpha$ relaxation of both blends gradually shift to a lower temperature and the apparent activation energy $\Delta E_\alpha$ increases. In PPVC/PP-*g*-MA blends, $\beta$ relaxation shifts to a higher temperature as the content of PP-*g*-MA increases from 0 to 20 wt % and then change unobviously for further varying content of PP-*g*-MA from 20 to 35 wt %. On the contrary, in the PPSC/PP-*g*-MA blends $\beta_1$ relaxation, the apparent activation energy $\Delta E_{\beta 1}$ and $\beta_2$ relaxation are almost unchanged with blend composition, while $\Delta E_{\beta 2}$ increases with an increase of PP-*g*-MA content. In the composition range studied, storage modulus $E'$ of both blends increases before $\alpha$ relaxation as content of PP-*g*-MA increases; however, the increment of $E'$ value for PPSC/PP-*g*-MA blends decreases progressively between $\beta_2$ and $\alpha$ relaxation with increasing temperature, but in the region the increment for PPVC/PP-*g*-MA blends is independent of temperature. The flexural properties of PPVC/PP-*g*-MA blend show more obvious improvement on PP than one of PPSC/PP-*g*-MA blends. Scanning electron micrographs of fracture surfaces of the blends clearly demonstrate two-phase morphology, viz. the discrete particles homogeneously disperse in the continuous phase, the main difference in the morphology between both blends is that the interaction between the particles and the continuous phase is stronger for PPVC/PP-*g*-MA than for PPSC/PP-*g*-MA blend. By the correlation of the morphology with dynamic and mechanical properties of the blends, the variation of the relaxation behavior and mechanical properties with the component structure, blend composition, vibration frequency, and as well as the features observed in these variation are reasonably interpreted. © 1996 John Wiley & Sons, Inc.

## INTRODUCTION

Although polypropylene (PP) is a widely used thermoplastic on account of its low cost and versatile properties including mechanical, working temperature, extraordinarily chemical, and stress-cracking resistance, it often fails in being used as extrusion coating to make composites because of hardly adhering with most of the polymers, especially polar polymers, due to its nonpolarity and crystallization. The situation calls for modification of PP. There are a variety of techniques for promoting adhesion of PP with other materials, such as surface treatment (thermal oxidation,[1] plasma,[2,3] corona discharge,[4,5] coating with a primer[6,7]), chemical modification,[8] adding an adhesion promoter between PP and adherend,[9,10] and blending modification.[11] Of these techniques, the first could not improve adhesion strength too much, the second is efficient but uneconomical, the third is complex in processing procedure and low efficiency, the last is efficient and economical if a suitable modifier is chosen. By using

* To whom correspondence should be addressed.
† Present address: Department of Chemical Engineering, TianJin Institute of Light Industry, TianJin 300222, P.R. China.

Journal of Applied Polymer Science, Vol. 62, 813–826 (1996)
 CCC 0021-8995/96/050813-14

the last technique, we modified PP with polypropylene grafted with maleic anhydride (PP-*g*-MA), which has low molecular weight and higher hardness, to improve the properties of PP and reduce its melt viscosity for the application of the extrusion coating. The experimental data have shown that the modified PP with PP-*g*-MA not only enhanced adhesiveness of PP with polar polymer but also mechanical properties.

This article presents a study of dynamic and mechanical properties of both homopolypropylene/maleated polypropylene and ethylene–propylene block copolymer/maleated polypropylene blends, and the correlation of the properties with the morphology of the blends. In this study PP is used as a matrix; the content of PP-*g*-MA in the blend varied from 0 to 50 wt %. The data for storage modulus $E'$ and loss tangent than $\delta$ as a function of temperature, covering a frequency range from 0.3 to 30 Hz, and flexural properties as a function of blend composition at 20°C, are displayed. The effects of component structure, blend composition, and vibration frequency on relaxation behavior of the blends are discussed in detail, and all these results regarding dynamic and mechanical properties are found to be consistent with the morphology for the blends studied.

## EXPERIMENTAL

### Materials

In this study, the polypropylene (PP) used was PP VC20 82C (homopolypropylene, $M_w/M_n$: 225,000/52,000) and PP SC13 11M (ethylene–propylene block copolymer, ethylene content in the copolymer: 6–13 wt %,[12] $M_w/M_n$: 265,000/58,000) produced by Borealis Polymers Co. Maleated PP used was supplied by Eastman Chemical Co. with the following specification: content of maleic anhydride (MA): 8–10 wt %, $M_w/M_n$: 9100/3900, ring ball and softening point: 157°C, viscosity (190°C): 400 cP. The three materials are abbreviated as PPVC for PP VC20 82C, PPSC for PP SC13 11M, and PP-*g*-MA for maleated PP.

### Preparation of Blends

Both PPVC/PP-*g*-MA and PPSC/PP-*g*-MA blends were prepared by melt mixing the component polymers, in the requisite rations, in the twin-screw extruder (Berstorff ZE 25*33D) at a screw speed of 150 1/min and the temperature zones (from feeding zone to the die): 210, 210, 220, 220, 220, 220, and 215°C. The strands obtained from the extruder were cut into small granules in a granulator. The samples used as the test of DMTA, flexural, and SEM were made according to the standard of the measurement.

### Measurement

The dynamic mechanical properties of the blends were determined using a dynamic mechanical thermal analyzer (Polymer Laboratories DMTA MKII). Owing to the fragility of the PP-*g*-MA sample at a low temperature, it is very difficult to prevent the sample from breaking. Therefore, the measurements were performed between −80 and 160°C for PP and blends, and from −20 to 140°C for PP-*g*-MA at fixed frequencies of 0.3, 1, 3, 10, and 30 Hz, and a heating rate of 2°C/min in both cases.

The flexural properties of the blends were tested according to ISO 178. The size of the samples was about 40 mm in length, 25 mm in width, and 2 mm in thickness; span used: 32 mm; speed of testing: 1 mm/min.

Differential scanning calorimetry (DSC) measurements of 10 mg samples were performed using a Perkin–Elmer DSC-7 apparatus in the first heating, cooling, and then second heating cycles at a rate

**Table I Melting and Crystallization Data of PPVC/PP-*g*-MA Blends**

| | $T_m$ (°C) | | $X_c$ (%) | | |
|---|---|---|---|---|---|
| PPVC/PP-*g*-MA | 1st Heating | 2nd Heating | 1st Heating | 2nd Heating | $T_c$ (°C) |
| 100/0 | 164.1 | 163.1 | 54.8 | 53.3 | 104.8 |
| 90/10 | 163.3 | 158.2 | 56.6 | 56.0 | 108.8 |
| 80/20 | 162.3 | 157.6 | 57.1 | 55.8 | 108.5 |
| 65/35 | 161.8 | [a] | 54.4 | 53.4 | 107.9 |
| 0/100 | 157.2 | 155.8 | 52.9 | 55.1 | 105.1 |

[a] A shoulder peak of melting occur at 155.4 and 161.2°C.

of 10°C/min. Crystallinity of the specimens was calculated according to

$$X_c(\%) = (\Delta H_m/\Delta H_m^\circ) \times 100$$

taking $\Delta H_m^\circ = 134$ J/cm$^3$.[13]

Morphology of the fracture surface of the samples after cooling in liquid nitrogen was studied by means of a scanning electron microscope (JEOL T100).

## RESULTS AND DISCUSSION

### Melting and Crystallization Behavior

Tables I and II show DSC data for both PPVC/PP-*g*-MA and PPSC/PP-*g*-MA blends in the first heating, cooling, and the second heating cycles at a rate of 10°C/min. It is observed that the melting point, $T_m$, of PP-*g*-MA is lower than the ones of both PPVC and PPSC, whereas the difference in crystallinity between both the PP-*g*-MA and the PP is very small. The lowering of $T_m$ for the PP-*g*-MA is understandable in light of the low molecular weight as well as a defect in the crystal[14] due to the presence of the MA groups. On the other hand, interaction of the anhydride groups and the low molecular weight make PP-*g*-MA favor crystallization. Therefore, the crystallinity of the PP-*g*-MA is almost the same as the one of PP, even though the anhydride groups that were grafted into molecular chains of polypropylene lead to the reduction in regularity of the chains.

Comparing both the PPVC and PPSC, as increasing PP-*g*-MA content, $T_m$ of both blends decreases slightly and the endothermic peak in the DSC curves of the blends shifts to a lower temperature (as shown in Tables I, II, and Fig. 1). It is an indication of the disappearance of the crystalline component with a high melt point, suggesting that addition of PP-*g*-MA leads to a reduction in the perfection of crystalline PP region. It is worth noting that crystallinity of both blends, especially when the blend ratios of PP to PP-*g*-MA are 90/10 and 80/20, is not lower than the matrix, and it might be attributed to the fact that during crystallizating the PP-*g*-MA with the low molecular weight in the blend improves the mobility of chains of the matrix polymer.

It is found that scanning times affects the shape of DSC curves of melting for both PPVC/PP-*g*-MA and PPSC/PP-*g*-MA blends; the 65/35 PPSC/PP-*g*-MA blend is an example (as shown in Fig. 2). In the first scanning, a single peak is presented in the curve. However, a shoulder or double peak occurs in the second scanning; the peak temperature of a lower temperature peak corresponds to that of the peak of melting for PP-*g*-MA, the peak temperature of a higher temperature peak is related with that of the peak of melting for PPSC, and it is a characteristic of a two-phase structure[15] in the crystalline region of the blend.

### Dynamic Mechanical Properties

#### *Effect of PP-g-MA*

Figure 3 and Tables III and VI show dynamic mechanical data of PPVC, PP-*g*-MA, and PPVC/PP-*g*-MA blends. Two relaxations in the tan $\delta$–$T$ (loss tangent vs. temperature) curve of PPVC are observed over the temperature range studied; a lower temperature relaxation between −20 and 30°C, which is relevant with $\beta$ relaxation, is attributed to the glass transition of the amorphous phase.[16–18] Another that appears near 80°C corresponds to $\alpha$ relaxation, which exists only in the presence of the crystalline phase.[19,20] $\beta$ and $\alpha$ relaxation of PP-*g*-MA occur at a lower temperature than the ones of PPVC, respectively. The drift of the $\alpha$ relaxation to the lower temperature suggests more defects in crystals of PP-*g*-MA. Laguna et al.[14] found that the microphotograph of PP grafted with maleic anhydride showed an imperfect and indistinct edge of

**Table II Melting and Crystallization Data of PPSC/PP-*g*-MA Blends**

| PPSC/PP-*g*-MA | $T_m$ (°C) | | $X_c$ (%) | | $T_c$ (°C) |
|---|---|---|---|---|---|
| | 1st Heating | 2nd Heating | 1st Heating | 2nd Heating | |
| 100/0 | 166.8 | 163.1 | 51.3 | 56.0 | 109.5 |
| 90/10 | 165.3 | 161.7 | 50.0 | 56.8 | 109.4 |
| 80/20 | 163.7 | 159.1 | 52.9 | 57.7 | 109.1 |
| 65/35 | 162.8 | [a] | 51.4 | 58.1 | 108.9 |
| 0/100 | 157.2 | 155.8 | 52.9 | 55.1 | 105.1 |

[a] A shoulder peak of melting occur at 156.8 and 162.4°C.

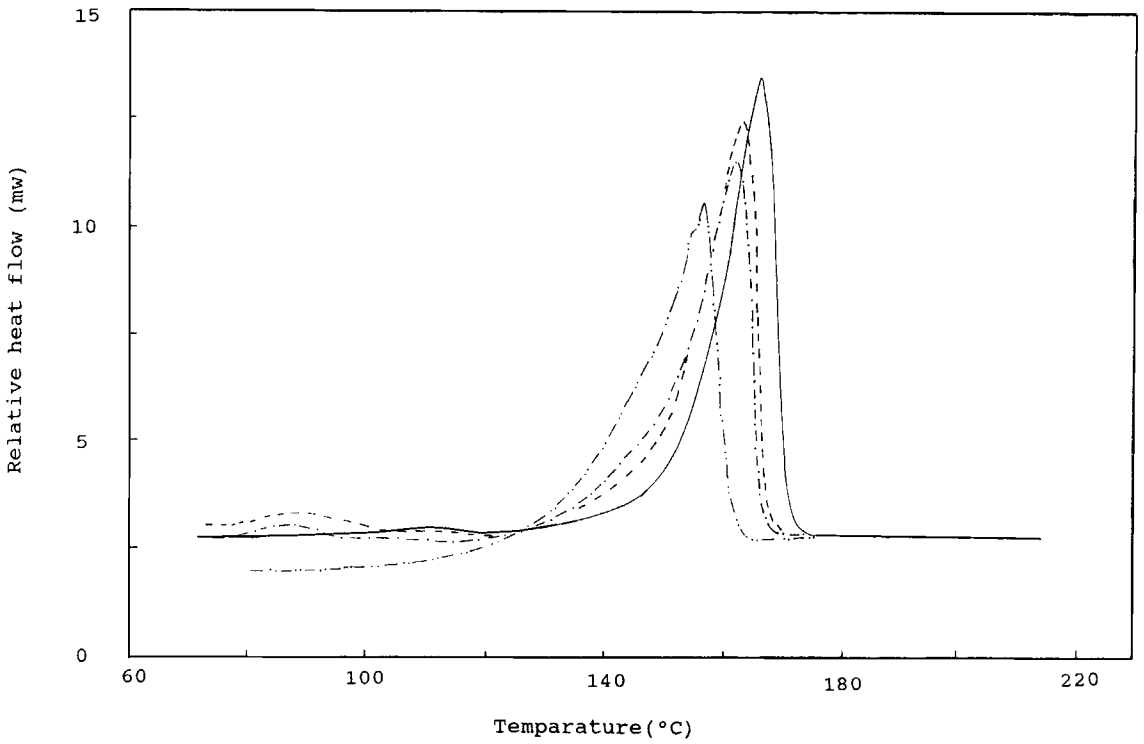


**Figure 1** DSC recordings for PSC/PP-*g*-MA blends at first heating and varying PP-*g*-MA content (wt %): (–).. 0; (– – –)?? 20; (– · –) 35; (– · · –) 100.

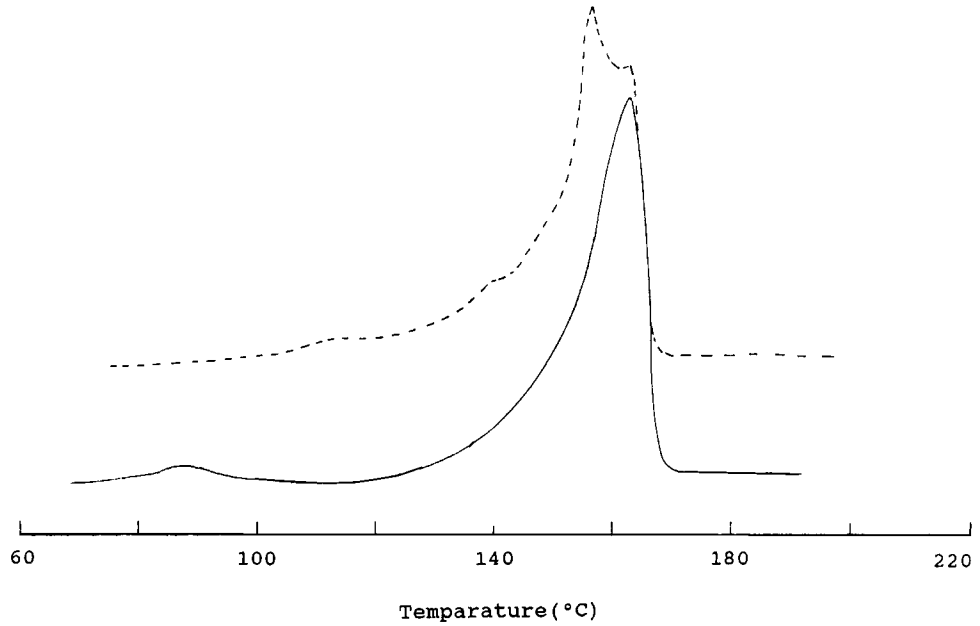


**Figure 2** Effect of scanning times on DSC pattern of 65/35 PPSC/PP-*g*-MA blend (heating rate 10°C/min): (–) first scanning; (– –) second scanning.

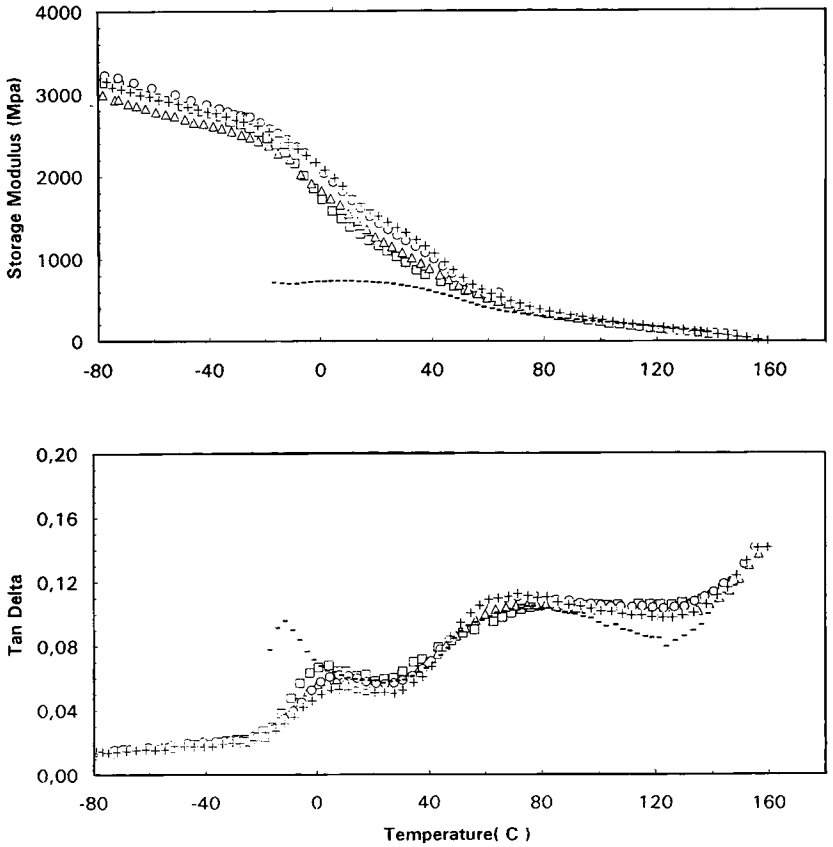


**Figure 3** $E'$ and tan $\delta$ as function of temperature for PPVC/PP-*g*-MA blends at 1 Hz and varying PP-*g*-MA content (wt %): (□) 0; (△) 10; (○) 20; (+) 35; (−) 100.

spheric crystal. Two factors might affect the $\beta$ relaxation of PP-*g*-MA: interaction of maleic anhydride groups that were grafted into molecular chains of polypropylene makes the $\beta$ relaxation shift to a higher temperature; the low molecular weight would cause the $\beta$ relaxation shift to a lower temperature; however, the latter might be dominating over the $\beta$ relaxation. In the blends of PPVC and PP-*g*-MA, $\beta$ relaxation shifts to a higher temperature as the content of PP-*g*-MA increases from 0 to 20%, and then the maximum temperature of $\beta$ relaxation increases no more as the content of PP-*g*-MA further increases from 20 to 35 wt %. On the other hand, the $\alpha$ relaxation shifts to a lower temperature and the peak

**Table III $\beta$ Relaxation Characteristics as a Function of Frequency for PPVC/PP-*g*-MA Blends**

| PPVC/PP-*g*-MA | | 30 Hz | 10 Hz | 3 Hz | 1 Hz | $\Delta E_\beta$[a] (kJ/mol) |
|---|---|---|---|---|---|---|
| 100/0 | $T$ (°C) | 10.6 | 7.8 | 5.1 | 2.4 | 273 |
| | tan $\delta_{max}$ | 0.091 | 0.073 | 0.069 | 0.068 | |
| 90/10 | $T$ (°C) | 14.9 | 11.9 | 9.5 | 6.9 | 290 |
| | tan $\delta_{max}$ | 0.083 | 0.066 | 0.059 | 0.059 | |
| 80/20 | $T$ (°C) | 15.8 | 13.3 | 10.5 | 7.8 | 288 |
| | tan $\delta_{max}$ | 0.083 | 0.067 | 0.061 | 0.062 | |
| 65/35 | $T$ (°C) | 14.2 | 13.4 | 10.6 | 7.8 | 334 |
| | tan $\delta_{max}$ | 0.075 | 0.058 | 0.052 | 0.053 | |

[a] Apparent activation energy.

**Table IV $\alpha$ Relaxation Characteristics as a Function of Frequency for PPVC/PP-*g*-MA Blends**

| PPVC/PP-*g*-MA | | 3 Hz | 1 Hz | 0.3 Hz | $\Delta E_\alpha$ (kJ/mol) |
|---|---|---|---|---|---|
| 100/0 | $T$ (°C) | 101 | 85 | 82 | 116 |
| | tan $\delta_{max}$ | 0.10 | 0.105 | 0.115 | |
| 90/10 | $T$ (°C) | 84.4 | 79.8 | 72.3 | 193 |
| | tan $\delta_{max}$ | 0.10 | 0.106 | 0.115 | |
| 80/20 | $T$ (°C) | 81 | 74.8 | 68.8 | 191 |
| | tan $\delta_{max}$ | 0.105 | 0.111 | 0.120 | |
| 65/35 | $T$ (°C) | 78 | 71.3 | 70.8 | 256 |
| | tan $\delta_{max}$ | 0.106 | 0.113 | 0.119 | |

height enhances with an increase of PP-*g*-MA content. It is very interesting in variation of storage modulus $E'$ with the temperature and blend composition. With increasing PP-*g*-MA content, storage modulus $E'$ of PPVC/PP-*g*-MA blends obviously increases before $\alpha$ relaxation, and the increment of $E'$ values is almost unchanged with temperature. After $\alpha$ relaxation, the $E'$–$T$ (storage vs. temperature) curves for all the blends tend to converge.

Dynamic mechanical data of PPSC, PP-*g*-MA, and PPSC/PP-*g*-MA blends are shown in Figure 4 and Tables V, VI, and VII. PPSC exhibits three relaxations; the lowest temperature relaxation (or $\beta_1$ relaxation) is due to segment motion of ethylene block in the block copolymer; near room temperature relaxation (or $\beta_2$ relaxation) assigns to segment motion of propylene block in the copolymer; a relaxation locates between 40 and 100°C. In comparison

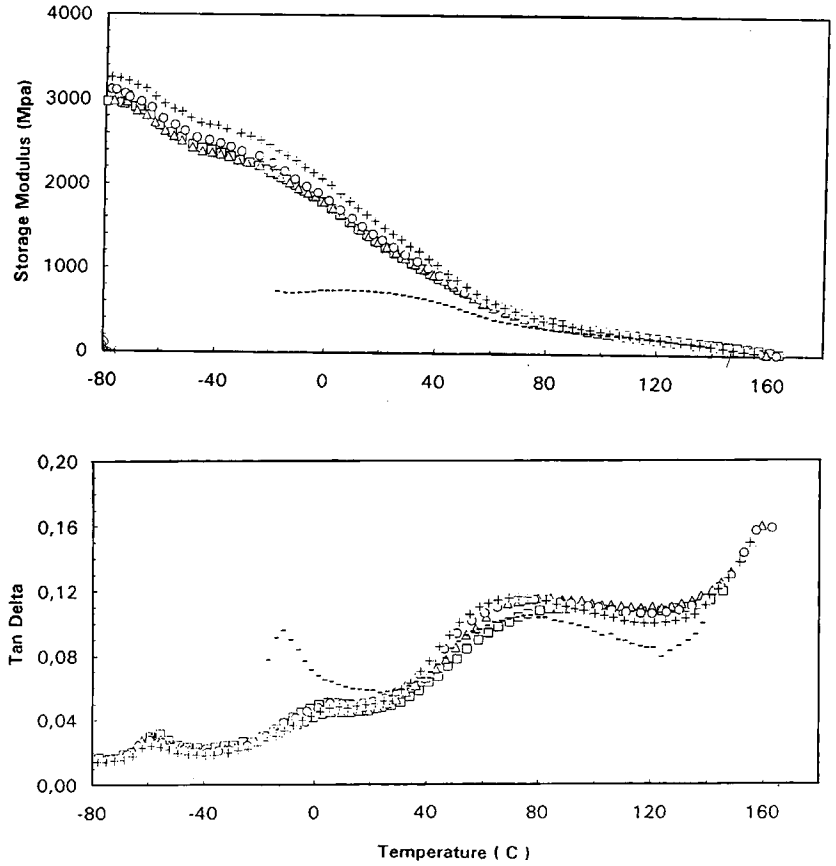


**Figure 4** $E'$ and tan $\delta$ as function of temperature for PPSC/PP-*g*-MA blends at 1 Hz and varying PP-*g*-MA content (wt %): (□) 0; (△) 10; (○) 20; (+) 35; (−) 100.

**Table V $\beta_1$ Relaxation Characteristics as a Function of Frequency for PPSC/PP-*g*-MA Blends**

| PPSC/PP-*g*-MA | | 30 Hz | 10 Hz | 3 Hz | 1 Hz | $\Delta E_{\beta 1}$ (kJ/mol) |
|---|---|---|---|---|---|---|
| 100/0 | $T$ (°C) | −51.5 | −53.5 | −56.5 | −58.5 | 198 |
| | tan $\delta_{max}$ | 0.053 | 0.038 | 0.032 | 0.031 | |
| 90/10 | $T$ (°C) | −52.5 | −55.7 | −56.9 | −58.6 | 221 |
| | tan $\delta_{max}$ | 0.053 | 0.037 | 0.031 | 0.030 | |
| 80/20 | $T$ (°C) | −51.6 | −54.8 | −65.4 | −59.1 | 184 |
| | tan $\delta_{max}$ | 0.059 | 0.035 | 0.029 | 0.028 | |
| 65/35 | $T$ (°C) | −54.2 | −54.5 | −58.6 | −59.6 | 198 |
| | tan $\delta_{max}$ | 0.047 | 0.032 | 0.026 | 0.025 | |

**Table VI $\beta_2$ Relaxation Characteristics as a Function of Frequency for PPSC/PP-*g*-MA Blends**

| PPSC/PP-*g*-MA | | 30 Hz | 10 Hz | 3 Hz | 1 Hz | $\Delta E_{\beta 2}$ (kJ/mol) |
|---|---|---|---|---|---|---|
| 100/0 | $T$ (°C) | 13.4 | 10.8 | 8.1 | 5.2 | 279 |
| | tan $\delta_{max}$ | 0.075 | 0.056 | 0.049 | 0.049 | |
| 90/10 | $T$ (°C) | 12.8 | 10.1 | 9.8 | 7.6 | 444 |
| | tan $\delta_{max}$ | 0.07 | 0.052 | 0.046 | 0.049 | |
| 80/20 | $T$ (°C) | 11.5 | 10.7 | 9.5 | 5.6 | 348 |
| | tan $\delta_{max}$ | 0.07 | 0.052 | 0.047 | 0.05 | |
| 65/35 | $T$ (°C) | 13 | 11 | 10.9 | 8.9 | 564 |
| | tan $\delta_{max}$ | 0.066 | 0.05 | 0.044 | 0.048 | |

**Table VII $\alpha$ Relaxation Characteristics as a Function of Frequency for PPSC/PP-*g*-MA Blends**

| PPSC/PP-*g*-MA | | 3 Hz | 1 Hz | 0.3 Hz | $\Delta E_{\alpha}$ (kJ/mol) |
|---|---|---|---|---|---|
| 100/0 | $T$ (°C) | 107 | 90.5 | 82.3 | 51 |
| | tan $\delta_{max}$ | 0.104 | 0.110 | 0.121 | |
| 90/10 | $T$ (°C) | 91.2 | 81.5 | 77 | 166 |
| | tan $\delta_{max}$ | 0.108 | 0.116 | 0.127 | |
| 80/20 | $T$ (°C) | 86.9 | 79 | 75.5 | 203 |
| | tan $\delta_{max}$ | 0.107 | 0.104 | 0.124 | |
| 65/35 | $T$ (°C) | 79.4 | 73.6 | 70.2 | 246 |
| | tan $\delta_{max}$ | 0.109 | 0.115 | 0.126 | |

with the PPVC/PP-*g*-MA blend, the regulars that the glass transition and storage modulus of PPSC/PP-*g*-MA blend vary with blend composition are different from the PPVC/PP-*g*-MA blend except for the $\alpha$ relaxation. As the content of PP-*g*-MA increases, $\beta_1$ and $\beta_2$ relaxation remains unchanged and storage modulus $E'$ increases only before $\alpha$ relaxation, while the increment of $E'$ values between $\beta_2$ and $\alpha$ relaxation decreases progressively with increasing temperature.

The above-mentioned results indicate that PP-*g*-MA added has an obvious effect on relaxation behavior of both PPVC/PP-*g*-MA and PPSC/PP-*g*-MA blends. On the basis of the data in melting and crystallization of both blends, the shift of $\alpha$ relaxation toward a lower temperature and the enhancement in the relaxation strength is attributed to defect movements in the crystalline region of the blends. The differences between PPVC/PP-*g*-MA and PPSC/PP-*g*-MA blends in relaxation behavior

assign to the difference in the two-phase structure that was formed after PP-*g*-MA was blended with two different structures of matrix, respectively. The explanation for this is given in relation to the morphology in a subsequent section.

### *Effect of Frequency*

As shown in Figures 5, 6, 7, and 8, variation of $E'$–$T$ and tan $\delta$–$T$ curves with vibration frequency for both blends are similar in shape. With an increase of frequency, $\beta$ and $\alpha$ relaxation of the blends shift to a higher temperature; there is a larger shift of maximum temperature for the $\alpha$ relaxation than for the $\beta$ relaxation, indicating that the apparent activation energy is larger for the $\beta$ than the $\alpha$ relaxation. It agrees well with the results shown in Tables III, IV, V, VI, and VII. On the contrary, the values of tan $\delta$ appear quite different, dependent on the frequency at different temperature ranges in tan $\delta$–$T$ curves. Before the $\alpha$ relaxation, the tan $\delta$ values are almost unchanged with an increase of frequency from 0.3 to 3 Hz and then an increase from 3 to 30 Hz. At the $\alpha$ relaxation region, tan $\delta$ values decrease as the frequency increases from 0.3 to 10 Hz, and the $\alpha$ peak disappears at 30 Hz. Therefore, the $\beta$ relaxation occurs at a higher frequency (or lower temperature); the $\alpha$ relaxation occurs at lower frequency (or higher temperature); it is consistent with the time–temperature equieffect principle.

According to Tables III, IV, V, VI, and VII, any increase in vibration frequency causes $\beta$ and $\alpha$ relaxation of the blends to shift to a higher temperature; the shift of the relaxation temperature allows one to calculate the apparent activation energy of the relaxation process for the blends, using the linear equation

$$\log f = \log f_0 + \Delta E/(2.303\ RT) \qquad (1)$$

where $f$ is the frequency, $f_0$ is a constant, $\Delta E$ is the apparent activation energy, $R$ is the gas constant, and $T$ is the absolute temperature corresponding to tan $\delta_{max}$. The values listed in these tables indicate

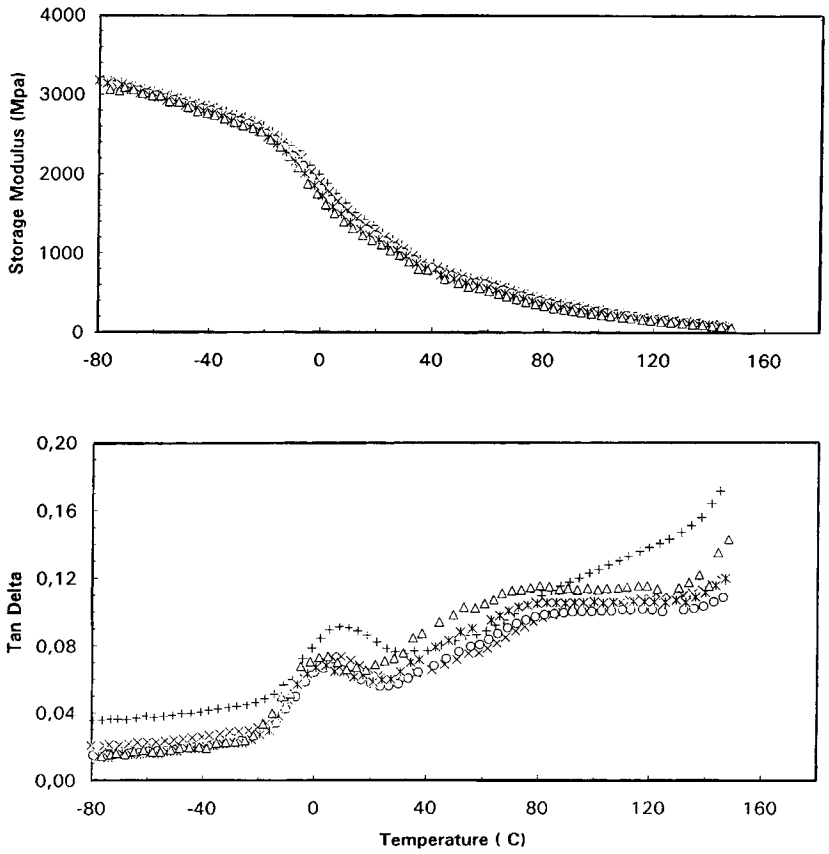


**Figure 5** $E'$ and tan $\delta$ as function of temperature for PPVC at (+) 30 Hz, (×) 10 Hz, (○) 3 Hz, (✳) 1 Hz, and (△) 0.3 Hz.

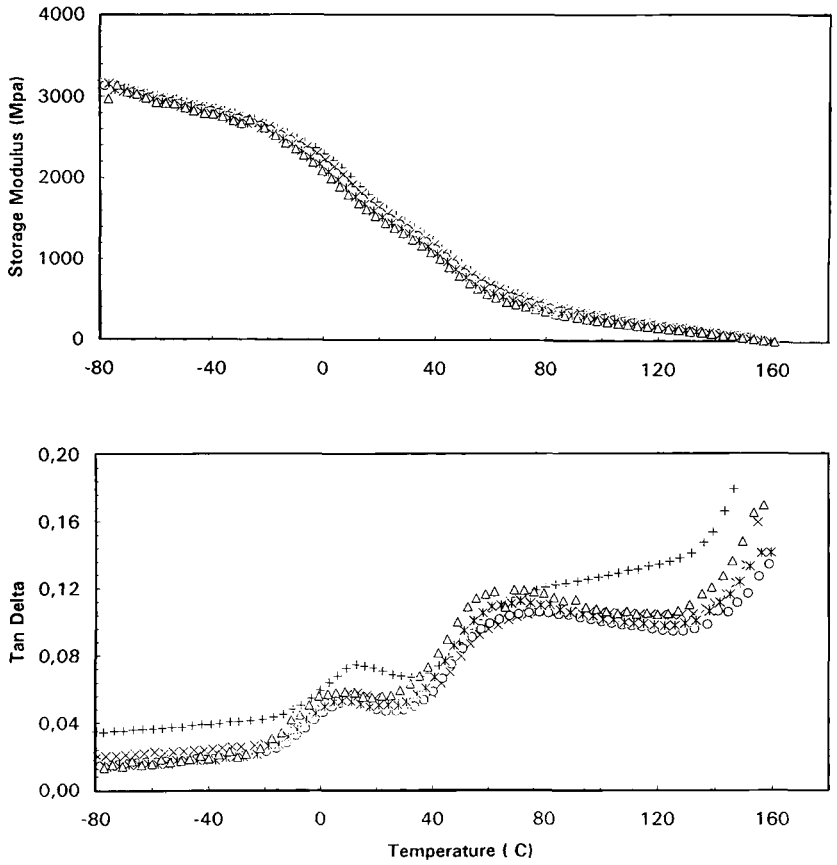


**Figure 6** $E'$ and tan $\delta$ as function of temperature for PPVC/PP-*g*-MA (65/35) blend at (+) 30 Hz, (×) 10 Hz, (○) 3 Hz, (✳) 1 Hz, and (△) 0.3 Hz.

that the apparent activation energy $\Delta E_\beta$ and $\Delta E_\alpha$ for PPVC/PP-*g*-MA blends increase with increasing PP-*g*-MA content. For PPSC/PP-*g*-MA blends, the variation of $\Delta E_{\beta 2}$ and $\Delta E_\alpha$ with blend composition is the same as the PPVC/PP-*g*-MA blends, but $\Delta E_{\beta 1}$ is not affected by the blend composition, suggesting poor interaction between ethylene block component in the copolymer and the PP-*g*-MA component.

## Flexural Properties

In thermoplastics, the flexural strength and modulus of PP is not high, and the deficiency would limit its application in many fields. Therefore, research and development of the engineering PP materials with good adhesiveness is attracting more and more interest. PP-*g*-MA is quite a brittle but hard wax; the flexural strain and modulus at 20°C are near 0.52% and 1024 MPa, respectively, and the properties show that it is very difficult to process by product alone. It was astonishing that PP-*g*-MA added in the PP resin had evidently improved flexural properties of PP (as shown in Table VIII). If we use a rule of mixture to judge blending effect, as follows

$$P = P_1 w_1 + P_2(1 - w_1), \qquad (2)$$

where $P_1$, $P_2$, and $P$ are the properties of PP, PP-*g*-MA, and blend, respectively, and $w_1$ is the weight fraction of PP component in the blend. The result indicates that the flexural strength, strain, and modulus as a function of PP-*g*-MA content for both blends demonstrate an obvious positive deviation from the values estimated from eq. (2). With increasing PP-*g*-MA content, the flexural modulus of both blends increase, the flexural strength and strain rise up to a maximum, and then fall. The maximum strength (or strain) of PPVC/PP-*g*-MA blend occurs at higher PP-*g*-MA concentration compared with the PPSC/PP-*g*-MA blend. On the other hand, the flexural strength, strain, and modulus are higher for

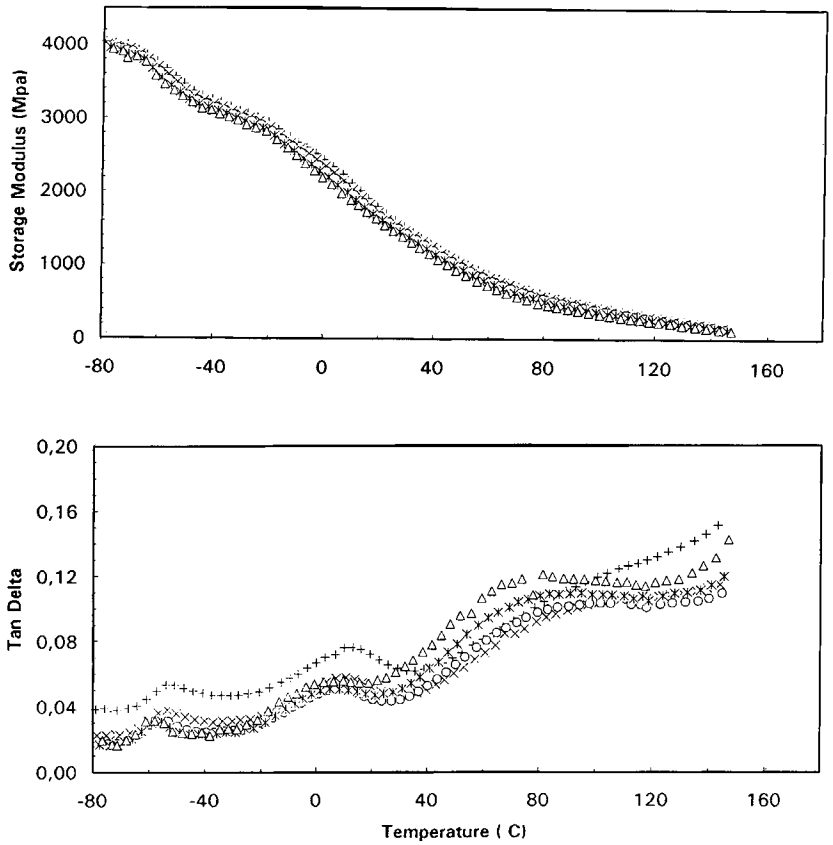


**Figure 7** $E'$ and tan $\delta$ as function of temperature for PPSC at (+) 30 Hz, (×) 10 Hz, (○) 3 Hz, (✳) 1 Hz, and (△) 0.3 Hz.

the PPVC/PP-*g*-MA than for the PPSC/PP-*g*-MA blend at the same blend composition.

The data indicate that PP-*g*-MA in the blends acts as an effect of toughening and reinforcing PP, especially in the PPVC/PP-*g*-MA blend. The former is attributed to the fact that PP-*g*-MA with low molecular weight has a function of plasticizing; thus, the strain of the blend is higher than that of PP at a suitable ratio of PP to PP-*g*-MA, but the fragility of PP-*g*-MA would appear if the PP-*g*-MA content in the blend is too high. Moreover, the reinforcing effect of PP-*g*-MA in the blends is due to interaction of the maleic anhydride groups of PP-*g*-MA molecular chains. The weak interfacial adhesion between PPSC and the PP-*g*-MA component in the blend causes the flexural properties of PPSC/PP-*g*-MA blend to be lower than that of the PPVC/PP-*g*-MA blend, and it is very coincident with the dynamic mechanical properties of both blends.

## Morphology and Its Correlation with Dynamic and Mechanical Properties

It is well known that crystallable PP, which consists of crystalline and amorphous regions, is a nonpolar polymer. PP-*g*-MA used in the study possesses high maleic anhydride content (8–10 wt % MA); the maleic anhydride groups grafted into PP molecular chains reduce its steric regularity and increase its polarity. The difference in structure between the PP and the PP-*g*-MA causes inevitably two-phase morphology in both crystalline and amorphous regions of the blends after PP-*g*-MA was melt blended with PPVC or PPSC. On the other hand, PP-*g*-MA in the blend leads to imperfect crystallization of the matrix; the higher content of PP-*g*-MA in the blend, the more obvious the situation is. Therefore, the $\alpha$ relaxation of the blends shifts to a lower temperature, and the relaxation strength enhances as PP-*g*-MA content increases.

Scanning electron micrographs of fracture surfaces of both PPVC/PP-*g*-MA and PPSC/PP-*g*-MA blends at varying blend composition are shown in Figures 9 and 10, respectively. These micrographs verify the two-phase morphology of the blends, which agrees with the result recently reported by González–Montiel et al.[21] using transmission electron micrography (TEM), i.e., discrete particles of PP-*g*-MA disperse in the continuous PP phase. The average diameter of particles (the number-average

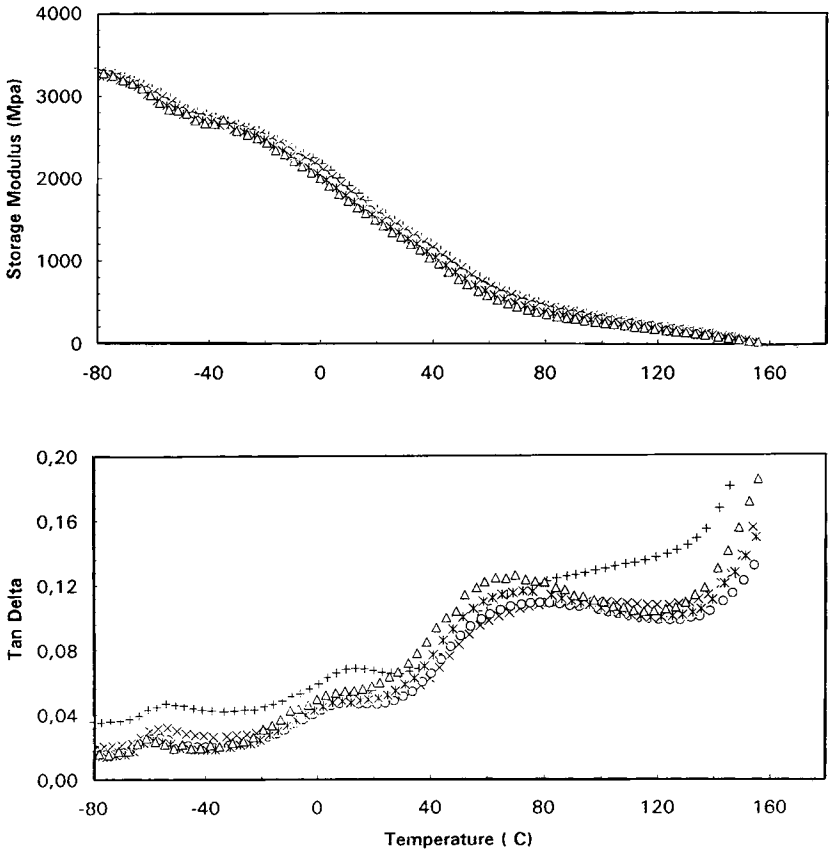


**Figure 8** $E'$ and tan $\delta$ as function of temperature for PPSC/PP-*g*-MA (65/35) blend at (+) 30 Hz, (×) 10 Hz, (○) 3 Hz, (✳) 1 Hz, and (△) 0.3 Hz.

diameter of the particles was calculated after measuring the diameter of 100 particles for each sample of the blend), when PP-*g*-MA content in blend is 10 and 20 wt %, is about 2.5 $\mu$m. The size of particle increases at 35 wt % PP-*g*-MA content due to coalescence of the particles. The interface between the particle and continuous phase is obscure for the both PPVC/PP-*g*-MA and PPSC/PP-*g*-MA blends, indicating adhesion between the two phases. Although it is quite difficult to discern the difference between the two blends from the micrographs, information about the difference in morphology between the two blends could be obtained from the dynamic mechanical spectra of the both blends. With increasing the PP-*g*-MA content, in the PPVC/PP-*g*-MA blend the $\beta$ relaxation shifts to a higher temperature,

**Table VIII Flexural Properties of Both PPVC/PP-*g*-MA and PPSC/PP-*g*-MA Blends**

| | Strength (MPa) | | Strain (%) | | Modulus (MPa) | |
|---|---|---|---|---|---|---|
| PP/PP-*g*-MA | A[a] | B[b] | A | B | A | B |
| 100/0 | 25.42 | 24.54 | 8.63 | 8.36 | 417 | 479 |
| 95/5 | 28.01 | 25.81 | 9.07 | 8.98 | 615 | 562 |
| 90/10 | 28.77 | 25.74 | 9.48 | 8.36 | 626 | 634 |
| 80/20 | 30.86 | 29.16 | 9.11 | 8.31 | 739 | 734 |
| 65/35 | 32.25 | 32.73 | 8.25 | 7.65 | 707 | 751 |
| 50/50 | 32.35 | 27.54 | 4.01 | 4.68 | 892 | 771 |
| 0/100 | 5.66 | | 0.52 | | 1024 | |

[a] PPVC/PP-*g*-MA blends.
[b] PPSC/PP-*g*-MA blends.

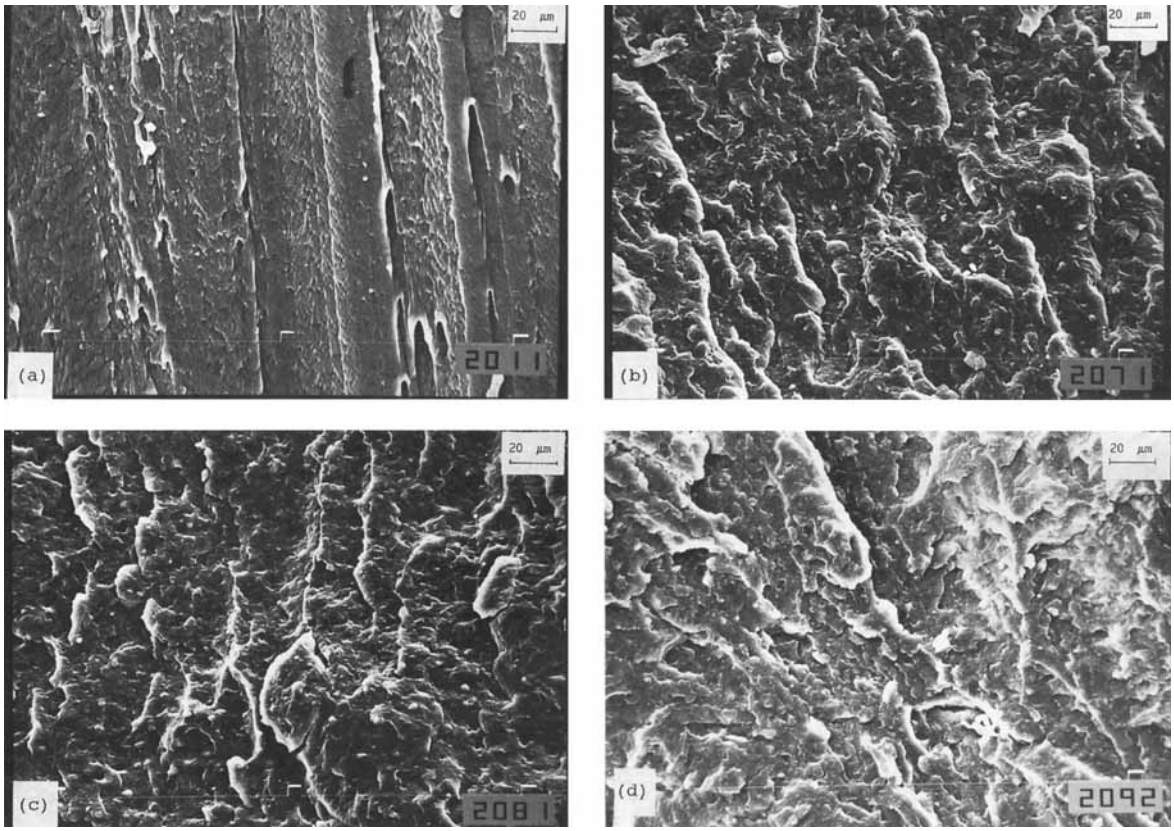


**Figure 9** Scanning electron micrographs of PPVC/PP-*g*-MA blends at varying composition (PP-*g*-MA content, wt %): (a) 0; (b) 10; (c) 20; (d) 35.

whereas the $\beta_1$ and $\beta_2$ relaxation, in the PPSC/PP-*g*-MA blend unobviously change. It suggests that interfacial interaction between the particle and the continuous phase is stronger for the PPVC/PP-*g*-MA than for the PPSC/PP-*g*-MA blend.

In view of the dynamic mechanical properties and the morphology of the both blends, it could be inferred that the maleic anhydride groups of PP-*g*-MA molecular chain in the particle of the blend might aggregate in a certain mode, which acts as physically crosslinking nodes. Thus, in the PPVC/PP-*g*-MA blend, the stronger interaction between the particle and continuous phase due to a more similar structure leads to $\beta$ relaxation shifts to a higher temperature and $E'$ values being larger for the blends than for pure PPVC, and increase with increasing PP-*g*-MA content before $\alpha$ relaxation. After $\alpha$ relaxation, the interaction of polar groups in the particles reduce because of higher temperatures, making the $E'$–$T$ curves converge. In the PPSC/PP-*g*-MA blend, the ethylene block of PPSC molecular chains is incompatible with the discrete particles, which slightly reduces interaction between the discrete particle and the continuous phase; therefore, the $\beta_1$ and $\beta_2$ relaxation unobviously change, and the flexural properties are better for the PPVC/PP-*g*-MA than for the PPSC/PP-*g*-MA blend.

## CONCLUSIONS

The dynamic mechanical analysis of both the PPVC/PP-*g*-MA and PPSC/PP-*g*-MA blends show that PP-*g*-MA in PP causes $\alpha$ relaxation shifts to lower temperatures and the relaxation strength enhances due to the defect movements in the crystalline region of the blends, while the relaxation behavior in the amorphous region of the blend are distinctly dominated by the matrix structure besides PP-*g*-MA: addition of PP-*g*-MA to PPVC makes $\beta$ relaxation shift to a higher temperature; $\beta_1$ and $\beta_2$ relaxation of PPSC, however, are almost unchanged with blend composition.

A significant improvement on the flexural properties for PP is observed due to addition of PP-*g*-MA, especially for PPVC. The flexural modulus of

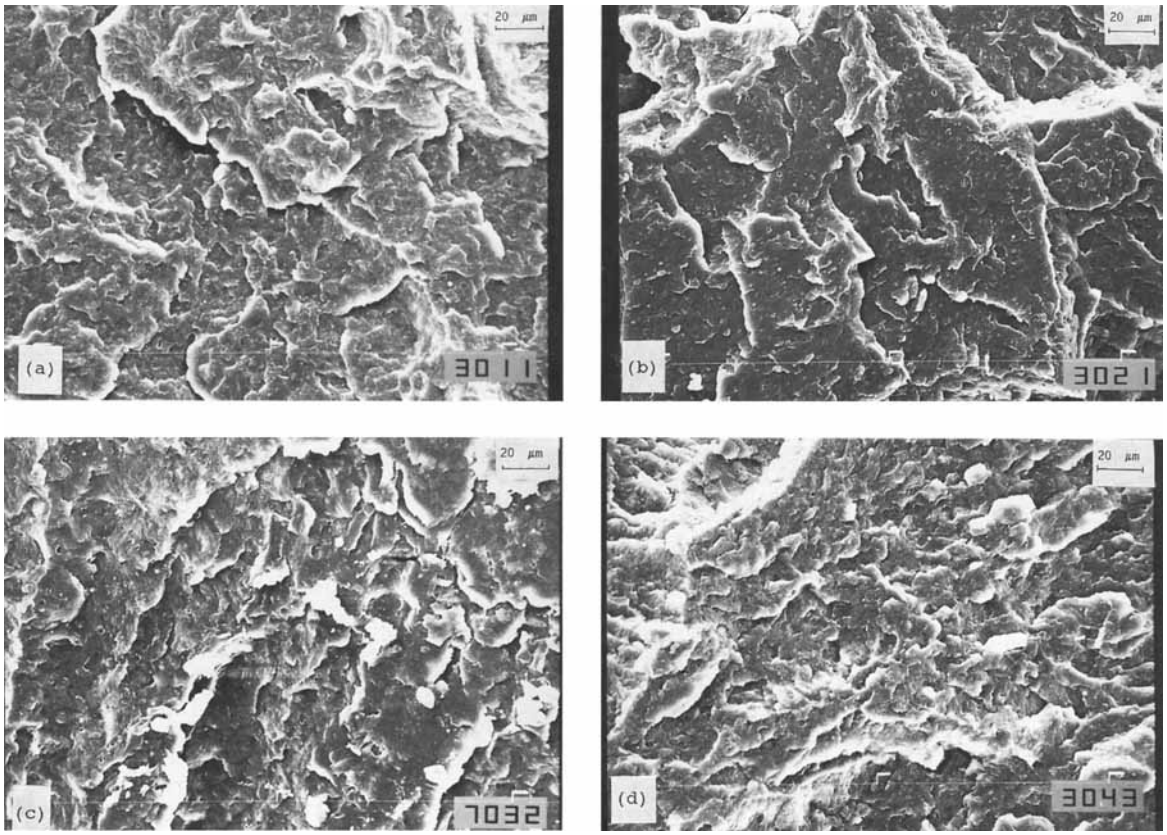


**Figure 10** Scanning electron micrographs of PPSC/PP-*g*-MA blends at varying composition (PP-*g*-MA content, wt %): (a) 0; (b) 10; (c) 20; (d) 35.

both blends increase with increasing PP-*g*-MA content; this is consistent with the data that storage modulus $E'$ in dynamic mechanical spectra of the blends increase with increase in PP-*g*-MA content. The maximum of the flexural strength and strain of the blend can be obtained in a appropriate blending ratio.

The scanning electron micrographs of the fracture surface of the samples show that PPVC/PP-*g*-MA and PPSC/PP-*g*-MA blends exist in two-phase morphology, viz. discrete particles of PP-*g*-MA disperse in the continuous PP phase in the composition range studied. The main difference in morphology for both blends is that the interfacial interaction between the discrete particle and the continuous phase is stronger for the PPVC/PP-*g*-MA than for the PPSC/PP-*g*-MA blend. By the correlation of the morphology with the dynamic and mechanical properties for the blends, it is deduced that the interaction of maleic anhydride groups in the particle acts as physically crosslinking nodes.

The authors are grateful to Neste Foundation for financial support. The authors also thank Mrs. Sinikka Pohjonen for her assistance in both the measurement of DMTA and the preparation of scanning electron micrographs.

## REFERENCES

1. D. Beiggs, D. M. Brewis, and M. B. Konieczk, *Eur. Polym. J.*, **14**, 1 (1978).
2. H. Yasuda, *Plasma Polymerization*, Academic Press, London, 1985.
3. C. M. G. Garlsson and G. Ström, *Surf. Interfal. Anal.*, **17**, 511 (1991).
4. D. Briggs, in *Surface Analysis and Pretreatment of Plastics and Metals*, Applied Science Publishers, England, 1982.
5. B. Westerlind, A. Larsson, and M. Rigdhl, *Int. J. Adhesion Adhesives*, **7**, 141 (1987).
6. C. Bonnerrup and P. Gatenholm, *J. Adhesion Sci. Technol.*, **7**, 247 (1993).
7. D. A. Tod, R. W. Atkins, and S. J. Shaw, *Int. J. Adhesion Adhesives*, **12**, 159 (1992).
8. M. M. Sain and B. V. Kokta, *Polym.-Plast. Technol. Eng.*, **31**, 89 (1994).
9. Jpn. Pat. 56144153 (1994).
10. Jpn. Pat. 05269914 (1993).

11. Jpn. Pat. 59223739 (1984).
12. H. Seppänen, personal communication, Jan. 30, 1996.
13. B. Pukanszky, K. Belina, A. Rockenbauer and F. H. J. Maurer, *Composites,* **25,** 205 (1994).
14. O. Laguna, J. P. Vigo, J. Taranco, J. L. Oteo, and E. P. Collar, *Rev. Plást. Mod.,* **56,** 878 (1988).
15. J. Duvall, C. Sellitti, C. Myers, A. Hiltner, and E. Baer, *J. Appl. Polym. Sci.,* **52,** 207 (1994).
16. J. A. Sauer, R. A. Wall, N. Fuschillo, and A. E. Woodward, *Appl. Phys.,* **29,** 1385 (1958).
17. N. G. McCrum, *Polym. Lett.,* **2,** 495 (1964).
18. I. Inamura, H. Ochiai, and H. Yamamura, *J. Polym. Phys. Ed., B,* **27,** 2267 (1974).
19. R. H. Boyd, *Polymer,* **26,** 323 (1985).
20. C. Jourdan, J. Y. Cavaille, and J. Perrez, *J. Polym. Sci., B,* **27,** 2361 (1989).
21. A. González-Montiel, H. Keskkula, and D. R. Paul, *J. Polym. Sci., B,* **33,** 1751 (1995).

*Received October 7, 1995*
*Accepted June 1, 1996*